RSC Advances

ROYAL SOCIETY OF CHEMISTRY

www.rsc.org/advances

Evaluation of *n*-butanol as an oxygenated additive to improve combustion-emission-performance characteristics of a diesel engine fuelled with diesel-calophyllum inophyllum biodiesel blend

S. Imtenan[1]; H.H. Masjuki; M. Varman; I. M. Rizwanul Fattah[2]

Centre for Energy Sciences, Faculty of Engineering, University of Malaya, 50603 Kuala Lumpur, Malaysia.

Abstract

Alexandrian laurel or *Calophyllum inophyllum* oil is considered as one of the most forthcoming non-edible biodiesel sources in recent years. In the present study, the relative improvement of Alexandrian laurel biodiesel-diesel blend (AL20) was attempted with the addition of 5-10% n-butanol (by vol.), which is often used as oxygenated cold starting additive. Constant 80 Nm torque at variable engine speed, ranging from 1000 to 3000 rpm was chosen as the operating condition on a 4-cylinder turbocharged, water cooled diesel engine. Brake specific fuel consumption (BSFC), brake specific energy consumption (BSEC) and brake thermal efficiency (BTE) was measured to compare the performance of the test fuels quantitatively. Engine emissions such as unburned hydrocarbons (HC), carbon monoxide (CO), nitrogen oxide (NO) and smoke opacity were also measured. Alcoholic oxygenated additives like n-butanol generally reduces the in-cylinder temperature. Therefore, in-cylinder pressures of the test fuels were acquired and the heat release rates (HRR) were analyzed to unveil the characteristics of the combustion mechanism. Correlation of performance and emission was made to the combustion parameters to obtain a better understanding of the scenario. However, in a nut-shell, the investigation exposes the potential of n-butanol to be used as the modifier of AL biodiesel-diesel blend in the context of combustion, performance and emission characteristics.

[1] Corresponding author. Tel.: +60146985294; Fax: +603 79675317 E-mail: sayeed.imtenan@gmail.com
[2] Corresponding author. Tel.: +60379674448; Fax: +603 79675317 E-mail: Rizwanul.buet@gmail.com

Keywords: Diesel-biodiesel blend; *n*-butanol; Calophyllum-inophyllum; Combustion; Engine performance-emission

1. Introduction

Biodiesel, which refers to the fatty acid alkyl esters (FAAEs), are derived from lipid constituents originated from vegetable oil, animal fats, waste greases, recycled cooking oils and other potential triacylglycerol-containing feedstocks [1]. In order to produce biodiesel, vegetable oils of edible source were treated as one of the potential feedstocks. However, due to high price of vegetable oil feedstocks obtained from traditional crops and food security concern, other sources like non-edible oils of plant origin, waste fats with high free fatty acid (FFA) content etc. are now being used for biodiesel production [2]. Now-a-days this is undisputed that, conventional diesel can be replaced by biodiesels to solve both of the concerns; energy crisis and legislative emission standards. Still, diesel can be replaced to some extent only by the oils of plant origin because, use of non-edible vegetable oils would not solve the competition for arable land between food production and transportation oil crop cultivation [3]. However, even with such trade-off, new target has been set for the European members by the European Renewable Energy Directive (RED) that, at least 10% biofuel have to be used on all forms of transport by 2020 [4-6]. Therefore, in the automotive fuel market, the share of biodiesel is going to be increased though it has some inherent disadvantages and complications. Higher density and viscosity, poor atomization and evaporation quality, advanced combustion and higher NOx emissions and poor cold flow properties etc. are the main problems regarding the use of biodiesels on diesel engines. Eradicating such problems

to make biodiesels more viable for the diesel engines is the key to modern biodiesel research works.

Alexandrian laurel (*Calophyllum inophyllum*) is a member of Clusiaceae or Guttiferae (mangosteen) family which is commonly known as Penaga Laut in Malaysia [7]. It is a medium-sized to large ornamental evergreen tree with a broad spreading crown of irregular branches and the average height is 8–20m [8]. The fruit is round and has a single large seed. Oil content of the kernels is almost 75% and the oil is non-edible. Fruits can be collected twice in a year and 18 kg of oil can be extracted from 100 kg of fruit [3]. Oil processing from Alexandrian laurel is not similar to the other vegetable oils. It forms during the nuts' desiccation. Without damaging the kernels, non-germinating ripe fruits are slightly crushed just to crack the shells. Then the kernels are exposed to the sun to desiccate. They become brownish, loose weight, develop aromatic odor and increase their oil content. Then oil can be extracted from the kernels [3]. It is native to East Africa, South, Southeast and East Asia, Australia, and the South Pacific where the weather is warm as well as wet or moderate and mean annual rainfall is around 1000-5000 mm [9]. Although the trees are vulnerable to fire and frost, they are extremely tolerant to strong wind, salt spray and brackish water tables [7]. The salt and wind withstanding ability makes it suitable for sand dune stabilization [10]. 400 tree/ha can be planted and usual oil yield is 4680 kg-oil/ha or 11.7 kg-oil/tree [11]. Therefore considering such huge agro-industrial potential, it has been widely planted throughout the tropics now. Growing interest on non-edible oils with high FFA content for biodiesel production has forced the researchers to draw attention towards AL (Alexandrian laurel) oil during the last decade [7, 12, 13]. However, very few studies can be found in the literature concerning AL biodiesel and most of those studies deal with biodiesel production process[10, 14-16]. Compatibility of 100% AL biodiesel or the blends with petroleum diesel in diesel engines in the context of performance and exhaust emissions has already been studied by

number of researchers. Venkanna and Reddy [17] tested variable percentage of AL biodiesel blended with diesel. They reported, up to 20% blend of AL biodiesel can be used in diesel engine without significant compromise of performance. However, for higher percentages, poor atomization was observed due to higher viscosity and density of AL biodiesel. In a different study the same authors studied the effect of injector opening pressure on engine performance running with AL biodiesel blends [18]. They reported that, the brake specific fuel consumption (BSFC) was increased with AL biodiesel for all the injector opening pressures compared to that of diesel. The higher density of AL biodiesel caused higher mass injection at all the injector opening pressures compared to diesel and increased the BSFC. Belagur and Chitimini [19] studied the effect of variable static injection timing on performance and emission of a single cylinder engine running by AL biodiesel. They worked out the best injection timing concerning the BSFC and brake thermal efficiency (BTE) values. However, BSFC value was still quite higher for AL biodiesel than that of neat diesel fuel. Rahman et al. [20] studied the performance and emission characteristics of AL biodiesel blends in four-cylinder diesel engine at high idling conditions. They also reported significantly higher BSFC values for AL biodiesel blends than diesel fuel. In addition, they found 20% blend of AL biodiesel produced the lowest amount of CO and HC emissions. Rizwanul et al. [21] studied 10-20% blend of AL biodiesel with diesel and reported higher BSFC, lower BTE for the biodiesel blends with higher NO_x emission. They pointed at higher density and viscosity of AL biodiesel for comparative poor performance. They also attributed higher molecular weight species of AL biodiesel for poor atomization in the premixed combustion region which certainly affected the combustion efficiency. Therefore, according to the literature, it is evident that, most of the researchers have found the higher density and viscosity of AL biodiesel responsible for comparatively poor performance characteristics.

Being a prospective non-edible renewable energy source, AL biodiesel deserves a profound investigation regarding its improvement in the context of performance and emission characteristics. Apart from blending it with petroleum biodiesel, which has already been tried by several researchers, one more suitable method to improve biodiesel performance is to use various kinds of cold starting additives having low density and viscosity to improve the fuel properties [4, 22, 23]. In recent times, *n*-butanol has appeared as a potential oxygenated additive to improve the fuel properties of both diesel and biodiesels [24-26]. *n*-butanol is also better known as 1-butanol, has a straight-chain structure and a OH group at the terminal carbon. It has less hydrophilic tendency, higher miscibility with diesel, higher cetane number and moderate calorific value [27, 28]. Yao et al. [29] studied the effect of *n*-butanol-diesel blend on the performance and emissions of a heavy-duty diesel engine with multi-injection and various exhaust gas recirculation (EGR) ratios. He reported that, the soot and CO emissions can be improved by the *n*-butanol addition without a serious compromise of the BSFC. There are quite a few studies regarding the blends of *n*-butanol and biodiesel or the blends of *n*-butanol-biodiesel-diesel [30-33] and the best advantage of these blends is that, the drawback of higher viscosity for the biodiesel and the lower cetane number for the *n*-butanol compared to biodiesel can be offsetted and more similar characteristics of diesel can be attained. Altun et al. [34] studied the effect of *n*-butanol on cottonseed biodiesel-diesel blend and reported that, emissions of NO_x , HC and CO reduced in expense of higher BSFC. Lebedevas et al. [35] investigated with butyl esters of rapeseed oil-diesel blend with the addition of 15-25% *n*-butanol and observed development on emission characteristics and overall efficiency. Mehta et al. [36] added variable percentage of *n*-butanol with jatropha biodiesel-diesel blend and reported significant drop in CO and NO emissions in expense of lower performance. However, a gap on the literature was found regarding the enhancement of combustion and engine performance-emission characteristics of AL biodiesel-diesel blend with the addition of

n-butanol. Therefore, the present investigation is an endeavour to improve the overall combustion, performance and emission characteristics of AL biodiesel-diesel blend with the addition of variable percentages of *n*-butanol.

2. Materials and method

2.1 Feedstock and additive

In this investigation crude AL oil was collected from local market. Biodiesel was produced from the crude oil and the procedure could be found from the work of the same authors [21]. *n*-butanol was purchased from Nacalai Tesque, Inc., Kyoto, Japan; certified as 99.5% pure. Petroleum diesel was supplied from the local market supplier.

2.2 Fatty acid composition (FAC)

In this investigation a gas chromatograph (Agilent 7890 Series, USA) equipped with flame ionization detector was used to explore the FAC of AL biodiesel. Table 1 and 2 show the GC operating conditions and the FAC results of the AL biodiesel. EN14103 standard was used to measure the total ester content and methyl linolenate content. On the contrary, EN 14105 standard was used to measure monoglyceride content, diglyceride content, triglyceride content, free and total glycerin content. It was observed that, AL biodiesel contains 29.3% saturated methyl esters, 40.5% mono-unsaturated methyl esters and 25.8% poly-unsaturated methyl ester.

Table 1 GC operating Condition for determination of fatty acid composition

Table 2 Fatty acid composition of AL biodiesel

2.3 Test fuels

The preparation of the test fuels and characterization of the properties were carried out at the Engine Tribology Laboratory, Department of Mechanical Engineering, University of Malaya. A total of four test fuels were selected for this investigation. The test fuels were (a) 100% petroleum diesel, (b) 20% AL biodiesel + 80% diesel (AL20), (c) 15% AL biodiesel + 5% *n*-butanol + 80% diesel (AL15B5), (d) 10% AL biodiesel + 10% *n*-butanol + 80% diesel (AL10B10). Volume based proportions were taken to blend the fuels. A blending machine rotating at 4000 rpm was used for 15-20 min to blend diesel and biodiesel. As *n*-butanol is volatile in nature, after addition of *n*-butanol, the blends were taken into a closed container and shaked with a shaker machine for about 30 min.

2.4 Equipment for fuel property test

Table 3 shows the list of the equipment used to measure the physicochemical properties of the base fuels (diesel and biodiesels) and fuel blends. The following equations were used to calculate the saponification number (SN), iodine value (IV) and cetane number (CN) of the biodiesel [37].

$$SN = \sum\left(\frac{560 \times Ai}{MWi}\right) \quad (1)$$

$$IV = \sum\left(\frac{254 \times D \times Ai}{MWi}\right) \quad (2)$$

$$CN = 46.3 + \left(\frac{5458}{SN}\right) - (0.225 \times IV) \quad (3)$$

Here, A_i = percentage of each component, D = number of double bonds, MW_i = mass of each component. Molecular weight of each component is given on Table 2.

Table 3 Equipment of fuel property test

2.5 Experimental setup

This investigation was performed using an inline four-cylinder, water-cooled, turbocharged, high speed diesel engine without any catalytic converter. Schematic diagram of the test setup is given on the Fig. 1. Engine specifications are listed in Table 4. An eddy current dynamometer, which can be operated at a maximum power of 250 kW was coupled to the engine. Measurement of HC, NO and CO emissions were conducted by Bosch BEA-350 exhaust gas analyzer. Smoke opacity was measured by Bosch RTM 430 smoke opacimeter. The method for measuring the HC and CO emissions was Non-dispersive infrared and the method for NO was electrochemical. Smoke opacity was measured by photodiode receiver method.

Engine performance and emission tests were carried out varying the engine speed ranging from 1000 to 3000 rpm at constant 80 Nm torque. For data acquisition, REO-DEC data control system was used, which was monitored with the help of REO-DCA software. Measured engine performance parameters of this investigation were BSFC (brake specific fuel consumption), BSEC (brake specific energy consumption) and BTE (brake thermal efficiency).

2.6 Combustion characteristics analysis

The test system was equipped with necessary sensors for combustion analysis. In-cylinder pressure was measured by using a Kistler 6058A type pressure sensor. It was installed in the combustion chamber through the glow plug port. Kistler 2614B4 type charge amplifier was

used to amplify the charge signal outputs from the pressure sensor. A high precision incremental encoder (2614A type) was used to acquire the top dead center (TDC) position and crank angle signal for every engine rotation. Simultaneous samplings of the cylinder pressure and encoder signals were performed by a computer with Dewe-30-8-CA data acquisition card. One hundred consecutive combustion cycles of pressure data were collected and averaged to eliminate cycle-to-cycle variation in each test. To reduce noise effects, Savitzky-Golay smoothing filtering was applied to the sampled cylinder pressure data. Other combustion parameters, such as heat release rate and start of combustion (SOC) were computed by using Matlab® R2009a software.

Heat release rate (HRR) analysis is the most effective way to gather information for the combustion mechanism in diesel engines. This method simplifies the identification of start of combustion (SOC) timing and differences in combustion rates from the HRR versus crank angle diagram [38]. Hence, HRR analysis is a significant parameter in understanding the combustion mechanism. Average in-cylinder pressure data of 100 consecutive cycles with a 0.1 crank angle (CA) resolution were used to calculate HRR. Analysis was derived from the first law of thermodynamics, as shown in Eq. (4), without taking heat loss into account through cylinder walls.

$$\frac{dQ}{d\theta} = \frac{V\frac{dP}{d\theta} + \gamma P\frac{dV}{d\theta}}{\gamma - 1} \qquad (4)$$

Where, $\frac{dQ}{d\theta} =$ rate of heat release (J/°CA), V = instantaneous cylinder volume (m^3), $\theta =$ crank angle (°CA), P = instantaneous cylinder pressure (Pa), $\gamma =$ specific heat ratio which is considered constant at 1.35 [39]

The input values are the pressure data and cylinder volume (with respect to crank angle). The V and $\frac{dV}{d\theta}$ terms are shown in the following equations:

$$V = V_c + A.\, r\,[1 - cos\,(\frac{\pi\theta}{180}) + \frac{1}{\lambda}\{\,1 - \sqrt{1 - \lambda^2\, sin^2\left(\frac{\pi\theta}{180}\right)}\,\}} \qquad (5)$$

$$\frac{dV}{d\theta} = (\frac{\pi A}{180}) \times r\,\{\,\sin(\frac{\pi\theta}{180}) + \frac{\lambda^2 sin^2(\frac{\pi\theta}{180})}{2 \times \sqrt{1-\lambda^2 sin^2(\frac{\pi\theta}{180})}}\,\} \qquad (6)$$

Here, $\lambda = \frac{l}{r}$ and $A = \frac{\pi D^2}{4}$, where l = connecting rod length, r = crank radius = 0.5 × stroke, D = cylinder bore, and V_c = clearance volume.

2.7 Accuracies and uncertainties

Uncertainty in the measurements may happen due to experimental conditions, equipment calibration, instrument selection and inaccuracies. Therefore, it is much needed to analyze the uncertainty of the measured values. Uncertainty of this experiment was analyzed through a study of the instruments' precision and accuracy (given on table 5) along with the repeatability of the tests using the similar method by Rizwanul Fattah et al. [21]. Experiments were performed several times, and data were collected at least three times. Average values were used for graph plotting.

Figure 1: Schematic diagram of the engine test bed

Table 4: Engine testbed equipment specification

Table 5 Measurement accuracy and uncertainty

3. Results and discussions

3.1. Fuel properties

Physicochemical properties of the base fuels and the blends are given in table 6 and 7 respectively. Each property was tested several times and then mean value was taken.

Table 6 Property of the base fuels

Table 7 Property of the fuel blends

Kinematic viscosity of the biodiesels depends of the fatty acid profile [42]. It can be seen from the Table 6 that, kinematic viscosity of the AL biodiesel is within the limit of ASTM-D6751 and EN 14214 standards. However, though AL biodiesel is meeting the standard, still it has got 36% higher value than the diesel fuel. From table 7 it can be seen that, addition of *n*-butanol reduced the value of kinematic viscosities of the modified blends at best 32% than AL biodiesel. It is most likely that, lower kinematic viscosity will assist the modified blends to get better atomization during the injection than the AL20 blend.

Density of the AL biodiesel was 4.7% higher than diesel fuel. However, blending with diesel (AL20) reduced the density slightly but addition of *n*-butanol reduced the density up to 4.3% than AL biodiesel. Therefore, as the portion of *n*-butanol increased, it reduced the density accordingly which made the values much similar to diesel fuel.

AL biodiesel has got quite lower (11.8%) calorific value than diesel. In addition, calorific value of *n*-butanol is even lower than the AL biodiesel. Consequently, though all the blends AL20, AL15B5 and AL10B10 showed lower calorific values than diesel, it was only 2.7% lower on average.

Flash point of the AL biodiesel was quite higher than diesel fuel. As the flash point of *n*-butanol was very low, modified blends showed lower flash points than AL20. However, according to ASTM D7467 standard, minimum range of flash point of the biodiesel blend is 52^0C. Therefore, in this study it can be said that all the fuels were safe to handle.

In tropical and hot countries of Asia, the cloud point and pour point values are of limited concern. But, it has much greater importance in countries where the weather is cold. From table 6, it can be seen that, cloud point and pour point of AL biodiesel was quite higher than the diesel. However, as the *n*-butanol is well accepted as the cold starting additive, it can be seen from the table 7 that, blends with *n*-butanol showed significantly lower cloud point and pour point values. This will permit the use of AL biodiesel even in cold weather with the addition of *n*-butanol. It can also be seen from table 6 that, AL biodiesel has higher cetane number compared to diesel. However, as the cetane number of *n*-butanol is quite lower, the modified blends are supposed to show lower cetane numbers compared to AL biodiesel blend.

3.2 Combustion characteristics

3.2.1 Analysis of in-cylinder pressure

In this study, the parameters used to compare the combustion scenario were in-cylinder pressure, heat release rate (HRR) and start of combustion (SOC). At constant 80 Nm torque, focusing on the 'hot' part around TDC (top dead centre), cylinder pressure against crank angle diagram at 2000 rpm for AL biodiesel blend and *n*-butanol blends are illustrated in Fig.2. Maximum cylinder pressure for all the test fuels occurred within the range of 8-9^{0}CA after top dead centre (ATDC). Peak in-cylinder pressure for diesel was 72.38 bar at 8^{0}ATDC which was maximum among the test fuels for the given operating condition. For AL20, maximum pressure was 70.23 bar at 8.5^0 ATDC. Generally, in diesel engines, maximum in-cylinder pressure largely depends on the fraction of burned fuel in the premixed combustion phase [43]. AL biodiesel consists higher molecular weight species and it resulted poor atomization before the premixed combustion phase [21]. Consequently, burned fuel fraction in

the premixed phase decreased for the AL20 and it represented lower in-cylinder pressure than diesel. With the addition of 5% *n*-butanol into the AL biodiesel-diesel blend, it was observed that the peak cylinder pressure increased and occurred a bit early than AL20. AL15B5 produced 71.34 bar maximum pressure at 8.2^0 ATDC. Slight higher in-cylinder pressure for this blend can be attributed to the lower viscosity and higher volatility of *n*-butanol which were conducive for more fuel-air mixture during the ignition delay period and resulted in higher premixed portion of combustion. However, as the percentage of *n*-butanol was increased to 10%, for AL10B10, peak pressure decreased and occurred slightly late than AL20. It showed 69.23 bar of maximum pressure at 9^0 ATDC. Lower in-cylinder pressure for AL10B10 can be attributed to the higher latent heat of evaporation and lower cetane number of *n*-butanol [44]. It can be explained more clearly by combining it to the HRR analysis of the corresponding fuel.

Figure 2 Cylinder pressure vs Crank angle diagram for *n*-butanol blends at 2000 rpm

3.2.2 Analysis of heat release rate

HRR analysis can explain the in-cylinder pressure characteristics of the fuels in a better way as it permits greater access to the combustion mechanism. Since, the engine has a pump-line-nozzle fuel injection system, advanced start of injection (SOI) can take place if the fuel is denser and has higher bulk modulus of compressibility (and vice versa). Therefore, instead of measuring the ignition delay, combustion scenario is described with the help of SOCs (start of combustion) here. Heat release rate of the test fuels at 80 Nm torque and 2000 rpm are given in the Fig. 3. It can be seen in the figure that, premixed combustion peak of the AL20 blend was quite lower than the diesel fuel, which actually led to comparatively lower

maximum pressure. SOC of the AL20 was observed at -3.3^{0}ATDC whereas for diesel it was at -3.5^{0}ATDC. Slight lower peak heat release rate was observed for AL20 because of the poor atomization and air-fuel mixing rate which in turn reduced the premixed air-fuel mixture. Also, higher density and viscosity of AL20 led to longer physical ignition delay and delayed the SOC slightly than diesel [45]. However, AL15B5 showed early SOC at -3.9^{0}ATDC and the premixed peak of the HRR was much higher and sharper than AL20. This higher HRR due to increased premixed combustion phase was actually translated into higher in-cylinder pressure for AL15B5 than AL20. Early SOC implies relatively faster evaporation of the fuel to create combustible charge in this case. On the contrary, for AL10B10, SOC was retarded at -3^{0}ATDC and the premixed peak was lower. Since, *n*-butanol has a lower cetane number and higher latent heat of evaporation, increasing its portion on the blend retarded SOC for comparatively higher ignition delay [4]. Higher latent heat of evaporation reduced the in-cylinder temperature during atomization and it is more likely that combustion occurred in a lower temperature environment produces lower HRR and in correspondence lower peak in-cylinder pressure. Since, current investigation was conducted in a turbocharged 4-cylinder engine; air-fuel ratio was very high. Therefore, it is obvious that, effect of lower temperature during the vaporization of the fuel was not significant enough for the 5% blend of *n*-butanol. However, 10% *n*-butanol helped to create significantly lower temperature during the vaporization of the fuel and delayed the SOC more than the other test fuels. In the mixing controlled zone, followed by the premixed combustion phase, both of the modified blends exhibited higher HRR than AL20. Since, fuel-air mixing velocity is the governing parameter of HRR in this zone, modified blends impulsively showed better results [39].

Figure 3 Heat release rate vs Crank angle diagram for *n*-butanol blends at 2000 rpm

3.3 Engine performance characteristics

3.3.1 Brake specific fuel consumption

In this study, for the assessment of the engine performance with different test fuels, brake specific fuel consumption (BSFC) was used as a convenient parameter as the test running condition was constant torque (80Nm) with variable speed ranging from 1000 rpm to 3000 rpm. BSFC indicates the ratio of fuel consumption rate to brake power output. It can be seen from the Fig. 4 that, BSFC of all the test fuels showed a decreasing trend as the engine speed was increased from 1000 rpm to 2000 rpm. Since, the injection pump of the test engine was distributor type, at low speed like 1000 rpm, delivered fuel quantity decreased which affected the atomization rate as well as the fuel-air mixing rate. Increasing the engine speed improved the scenario and in turn declined the BSFC. However, increment of BSFC after 2000 rpm can be attributed to the decreased volumetric efficiency during the higher speeds [46]. AL20 and its modified blends with *n*-butanol showed reasonably higher BSFC than diesel on average. AL20 showed on average 10.7% increment of BSFC than diesel. AL15B5 and AL10B10 showed better BSFC results than AL20. They showed on average 2.4% and 4.2% decrement of BSFC than AL20 respectively. Reason behind for the higher BSFCs of the AL biodiesel blend and its modified blends than diesel is the comparatively lower energy content of the blends. Per unit mass heating values of the blends were lower, therefore, consumption had to be higher to attain the constant 80 Nm torque. However, *n*-butanol blends showed lower BSFCs than AL20 though they got comparatively lower heating values. It actually indicates better combustion efficiency of the blends due to their high oxygen content, lower viscosity and density [44]. As the viscosity and density of AL20 was higher than its modified blends, adhesion of fuel in the cylinder wall due to higher spray penetration might happen for improper atomization. Therefore, these results surely indicate improvement of atomization of the modified blends.

Figure 4 BSFC vs speed diagram for AL biodiesel and its modified blends at 80 Nm torque

3.3.2 Brake specific energy consumption

Brake specific energy consumption (BSEC) is a tool for comparing the performance of fuels with different heating values. It is the product of the BSFC and heating value of fuel. It measures how much energy is being consumed in one hour to develop a unit power output. Usually, BSEC decreases with an increase in energy consumption efficiency [47]. Fig.5 illustrates the BSECs of the test fuels at different engine speeds at constant 80 Nm engine torque. It can be seen that, AL20 gave the highest BSEC, which was on average 8% higher than diesel. However, modified blends with *n*-butanol showed lower BSECs compared to AL20. AL15B5 and AL10B10 showed on average 3% and 5.8% decrement of BSEC than AL20 respectively. It can be seen that, increment of the percentage of *n*-butanol decreased the BSEC. Such decrement can be attributed to their higher combustion efficiency due to higher oxygen content and lower density and viscosity which in-turn improved atomization [25].

Figure 5 BSEC vs speed diagram for AL biodiesel and its modified blends at 80 Nm torque

3.3.3 Brake thermal efficiency

Brake thermal efficiency (BTE) measures the efficiency of the conversion of chemical energy into useful work in an engine. Dividing the useful work by the heating value of the fuel is the way to calculate BTE. Fig.6 shows the BTEs of the test fuels at different speeds with a constant 80 Nm torque. It can be seen that, AL20 exhibited lowest BTE among the fuels and

it was on average 23.8%. On the other hand, modified blends of AL biodiesel, AL15B5 and AL10B10, improved BTE than AL20 on average 3.2% and 6.3% respectively. Reasons for the improvement of BTEs of the modified blends are totally analogous to the reasons of improving the BSECs.

Figure 6 BTE vs speed diagram for AL biodiesel and its modified blends at 80 Nm torque

3.4 Engine emission characteristics

3.4.1 Nitrogen oxide emission

NO emission for the test fuels are illustrated in the Fig.7. Formation of NO inside the cylinder is generally governed by the mechanisms named thermal (Zeldovich), N_2O pathway, prompt (Fenimore), NNH mechanism and the fuel bound nitrogen [21, 44]. However, for a given fuel and operating condition NO formation generally depends on some physical factors like oxygen concentration, residence time, in-cylinder temperature and air surplus coefficient. In this study, AL20 produced 13.7% higher NO emission than diesel on average. Higher NO for AL20 can be attributed to higher molecular weight species and higher fuel bound oxygen. Higher molecular weight species burn in late combustion phases due to reduced atomization before premixed combustion. Therefore, higher oxygen content together with late phase combustion resulted in higher temperature and increased NO emission for AL20 [21, 48]. However, AL15B5 showed even higher NO emission (6.7%) than AL20. Higher oxygen content of the modified blend was the most probable cause for such higher emission of NO. Again, due to lower viscosity, density and higher volatility of *n*-butanol, premixed part of combustion (see Fig. 3) increased for AL15B5 and consequently NO emission increased because NO forms there mostly [4, 49]. On the contrary, increased portion of *n*-butanol

(AL10B10) reduced NO emission than AL20 about 8% on average primarily due to higher latent heat of evaporation of *n*-butanol [25, 50]. It is evident that, on the case of 5% blend the effect of higher oxygen content and higher premixed combustion was dominant while for 10% blend amount of *n*-butanol was good enough to create lower in-cylinder temperature which has been shown by other researchers for other fuels [34]. For higher latent heat of evaporation, in cylinder temperature and the premixed peak of the combustion was reduced (validated by comparative lower in-cylinder pressures) for the 10% blend of *n*-butanol. Consequently, NO emission of AL10B10 reduced.

Figure 7 NO emission vs speed diagram for AL biodiesel and its modified blends at 80 Nm torque

3.4.2 Carbon monoxide emission

An overly lean or an overly rich mixture are the two ways CO can be formed. In overly lean mixtures, flame cannot propagate through it and fuel pyrolysis with partial oxidation causes CO emission. For the overly rich mixture, the fuel cannot mix with sufficient amount of air and even if they mix, they do not get enough time to oxidize [51]. However, generally in diesel engines, CO forms at rich air–fuel mixture areas because of unavailability of oxygen to completely oxidize all CO content in the fuel. In Fig. 8, emission of CO for the test fuels has been shown at variable engine speed maintaining constant 80 Nm torque. For all the test fuels, up to 2000 rpm, emission reduced and afterwards increased slightly. Initially, increment of speed increased the in-cylinder temperature which assisted the CO oxidation, however, later on higher speeds than 2000 rpm may be reduced the availability of time required for oxidation mechanism [49]. AL20 produced quite a reduced emission compared to diesel all over the speed range. About 21% decrement on average was noticed for AL20 than

diesel. It can be attributed to higher oxygen content of biodiesel which assisted to achieve more complete combustion [21]. Another explanation which can be mentioned here is the lower carbon/hydrogen (C/H) ratio possessed by biodiesel than diesel fuel [21]. It was similarly assisting to produce lower CO emission. However, modified blends reduced the emission even better. AL15B5 and AL10B10 reduced the CO emission than AL20 about 19% and 26%, respectively because of more oxygen content [35]. Therefore, lower density and viscosity of the modified blends improved spray atomization and reduced fuel rich regions. On top of that higher oxygen content surely assisted complete oxidation of the fuels and reduced CO emission.

Figure 8 CO emission vs speed diagram for AL biodiesel and its modified blends at 80 Nm torque

3.4.3 Hydrocarbon emission

In Fig. 9 HC emissions from the test fuels are shown at the selected engine test operating condition. One of the major reasons of HC emission from diesel engines is fuel trapping in the crevice volumes of the combustion chamber. Incomplete fuel evaporation, locally over-lean or over-rich mixture and liquid wall films for excessive spray impingement are also have been stated as important factors [39]. However, AL20 reduced HC emissions significantly than diesel fuel. It gave about 25.3% decreased emission than diesel on average. Higher oxygen content of biodiesel enhanced the amount of hydrocarbon oxidation and reduced the emission. On the other hand, AL15B5 and AL10B10 showed 30% and 48% increment of HC emission than AL20 on average. Due to even higher oxygen content of *n*-butanol, HC emission was supposed to be reduced for the modified blends. However, slip of fuel out of the cylinder especially at low speed during expansion stroke might be the reason for such higher emission as additive like *n*-butanol having higher volatility made fuel evaporation

easier [50]. Again, turbocharged diesel engine inherently creates a homogeneous charge. Therefore, addition of *n*-butanol may create lean outer flame zone and increase HC emissions. Lean outer flame zone is actually the envelope of the spray boundary where because of over-mixing the fuel is already beyond the flammability limit [44]. Over-mixing is a common scenario during the combustion of the fuels with such additive as the lower density and viscosity certainly affect the mixing process.

Figure 9 HC emission vs speed diagram for AL biodiesel and its modified blends at 80 Nm torque

3.4.4 Smoke opacity

Smoke opacity indicates the soot content on the exhaust gas which is one of the main components of particulate matter. Hence, this parameter can be associated with fuels propensity to form particulate matter during combustion. Figs.10 illustrates the exhaust smoke opacity of the test fuels. AL20 gave about 6.1% decreased smoke opacity than diesel fuel. Soot formation takes place generally at the initial premixed combustion phase when the fuel-air equivalence ratio remains near to the stoichiometry. Therefore, higher oxygen content of AL20 provided oxygen in the fuel rich zones and reduced smoke opacity [46]. AL15B5 and AL10B10 also followed the trend of AL20. They showed on average 14% and 21% lower smoke opacity respectively as they were more oxygenated. Higher viscosity and density of AL20 made higher spray penetration during injection and that may resulted in incomplete oxidation in the center of fuel jets. However, the modified blends avoided the reason due to

comparatively lower density and viscosity and reduced the smoke opacity than AL20. Therefore, it is obvious that such oxygenated blends reduce the probability of rich fuel zone formation and assist to decrease the soot emission.

Figure 10 Smoke opacity vs speed diagram for AL biodiesel and its modified blends at 80 Nm torque

4. Conclusion

Alexandrian laurel is a potential non-edible source of biodiesel. In this investigation, comparative improvement of combustion, performance and exhaust emission characteristics of AL biodiesel blend (AL20) was studied with the addition of *n*-butanol at different percentages in a high-speed, water cooled turbocharged diesel engine. Based on the experimental investigation, the following conclusions can be made.

- Incremental addition of *n*-butanol reduced the density and viscosity of the diesel-biodiesel blend chronologically. In spite of lower calorific value of *n*-butanol and AL biodiesel, blends showed insignificant (3% on average) difference of calorific values than diesel fuel.
- AL20 showed 10.7% higher BSFC than diesel because of lower calorific value and inferior atomization quality. However, *n*-butanol blends showed 3.3% decreased BSFC than AL20 on average because of higher combustion efficiency owing to higher oxygen content, lower density and viscosity of *n*-butanol. BSEC and BTE values of modified blends were also promising indicating higher combustion efficiency.
- AL20 produced about 13.7% higher NO than diesel. 5% *n*-butanol blend showed slight higher NO emission than AL20 due to higher oxygen content. However, 10%

blend reduced NO emission due to comparatively lower temperature environment during combustion. On average 8% lower NO emission was observed for 10% *n*-butanol.

- AL20 showed about 21% decrement of CO emission than diesel. AL15B5 and AL10B10 showed even better results by reducing CO emission by 19% and 26% respectively than AL20 due to higher oxygen content. Regarding HC emission, though AL20 showed 25.3% decrement on average than diesel, modified blends showed 39% increment of emission than AL20. Due to slip of fuel out of the combustion chamber for the evaporative nature of *n*-butanol, HC emission increased for the modified blends.
- Smoke opacity was also reduced for AL20 about 6.1% than diesel. *n*-butanol blends reduced the smoke opacity about 17% than AL20 on average. Higher oxygen content of *n*-butanol provided sufficient oxygen even in fuel rich zones for the oxidation of soot.

Therefore, regarding performance and emission characteristics, 10% blend of *n*-butanol showed higher improvement than 5% blend. Since, the addition of *n*-butanol into the diesel-biodiesel blend improved the performance and emission characteristics of an engine, its use can be considered as an auspicious way to solve intrinsic problems with the usage of Alexandrian laurel biodiesel at aforementioned operating condition.

Acknowledgement:

The authors would like to appreciate University of Malaya for financial support through High Impact Research grant titled: “Clean Diesel Technology for Military and Civilian Transport Vehicles’’ having grant number UM.C/HIR/MOHE/ENG/07.

Reference:

1. G. Knothe, L. F. Razon and F. T. Bacani, *Industrial Crops and Products*, 2013, **49**, 568-572.
2. E. Dinjus, U. Arnold, N. Dahmen, R. Höfer and W. Wach, *Sustainable Solutions for Modern Economies*, 2009, 125.
3. A. Dweck and T. Meadows, *International journal of cosmetic science*, 2002, **24**, 341-348.
4. D. C. Rakopoulos, *Fuel*, 2013, **105**, 603-613.
5. E. F. B. Policy, in *Transportpolicy.net*, 2014.
6. E. Parlament and E. Rat, *Amtsblatt der Europäischen Union vom*, 2009, **5**, 2009.
7. H. C. Ong, T. M. I. Mahlia, H. H. Masjuki and R. S. Norhasyima, *Renewable and Sustainable Energy Reviews*, 2011, **15**, 3501-3515.
8. J. Friday and D. Okano, *Species Profiles for Pacific Island Agroforestry*, 2006, **2**, 1-17.
9. J. Friday and D. Okano, *Hawaii, USA: Permanent Agriculture Resources (PAR)*, 2006.
10. P. K. Sahoo, L. M. Das, M. K. G. Babu and S. N. Naik, *Fuel*, 2007, **86**, 448-454.
11. M. Mohibbe Azam, A. Waris and N. Nahar, *Biomass and Bioenergy*, 2005, **29**, 293-302.
12. A. E. Atabani, A. S. Silitonga, H. C. Ong, T. M. I. Mahlia, H. H. Masjuki, I. A. Badruddin and H. Fayaz, *Renewable and Sustainable Energy Reviews*, 2013, **18**, 211-245.
13. H. C. Ong, A. S. Silitonga, H. H. Masjuki, T. M. I. Mahlia, W. T. Chong and M. H. Boosroh, *Energy Conversion and Management*, 2013, **73**, 245-255.
14. P. Sahoo, L. Das, M. Babu, P. Arora, V. Singh, N. Kumar and T. Varyani, *Fuel*, 2009, **88**, 1698-1707.
15. B. K. Venkanna and C. Venkataramana Reddy, *Bioresource Technology*, 2009, **100**, 5122-5125.
16. V. SathyaSelvabala, D. K. Selvaraj, J. Kalimuthu, P. M. Periyaraman and S. Subramanian, *Bioresource Technology*, 2011, **102**, 1066-1072.
17. B. K. Venkanna and C. V. Reddy, *International Journal of Green Energy*, 2012, null-null.
18. B. K. Venkanna and C. Venkataramana Reddy, *Environmental Progress & Sustainable Energy*, 2013, **32**, 148-155.
19. V. K. Belagur and V. R. Chitimini, *International Journal of Ambient Energy*, 2012, **33**, 65-74.
20. S. M. A. Rahman, H. H. Masjuki, M. A. Kalam, M. J. Abedin, A. Sanjid and H. Sajjad, *Energy Conversion and Management*, 2013, **76**, 362-367.
21. I. M. Rizwanul Fattah, M. A. Kalam, H. H. Masjuki and M. A. Wakil, *RSC Advances*, 2014, **4**, 17787-17796.
22. T. Kannan and R. Marappan, *Journal of Applied Sciences*, 2011, **11**, 2961-2967.
23. F. Lujaji, A. Bereczky, C. Novak and M. Mbarawa, Proceedings of the World Congress on Engineering, 2010.
24. C. D. Rakopoulos, A. M. Dimaratos, E. G. Giakoumis and D. C. Rakopoulos, *Applied Energy*, 2011, **88**, 3905-3916.
25. D. Rakopoulos, C. Rakopoulos, E. Giakoumis, A. Dimaratos and D. Kyritsis, *Energy Conversion and Management*, 2010, **51**, 1989-1997.
26. E. Sukjit, J. Herreros, K. Dearn, R. García-Contreras and A. Tsolakis, *Energy*, 2012, **42**, 364-374.
27. A. C. Hansen and D. C. Kyritsis, *Biomass to Biofuels: Strategies for Global Industries*, 2010, 1-26.
28. M. S. Agathou and D. C. Kyritsis, *Fuel*, 2011, **90**, 255-262.
29. M. Yao, H. Wang, Z. Zheng and Y. Yue, *Fuel*, 2010, **89**, 2191-2201.
30. D. C. Rakopoulos, C. D. Rakopoulos, D. T. Hountalas, E. C. Kakaras, E. G. Giakoumis and R. G. Papagiannakis, *Fuel*, 2010, **89**, 2781-2790.

31. Y. Liu, W. Cheng, M. Huo, C. Lee and J. Li, ILASS-Americas 22nd annual conference on liquid atomization and spray systems, Cincinnati, OH, 2010.
32. T. Laza, R. Kecskés, Á. Bereczky and A. Penninger, *Periodica Polytechnica, Mechanical Engineering*, 2006, **50**, 11-29.
33. H. Liu, C.-f. Lee, M. Huo and M. Yao, *Energy & fuels*, 2011, **25**, 1837-1846.
34. S. e. Altun, C. Öner, F. Yaşar and H. Adin, *Industrial & Engineering Chemistry Research*, 2011, **50**, 9425-9430.
35. S. Lebedevas, G. Lebedeva, E. Sendzikiene and V. Makareviciene, *Energy & Fuels*, 2010, **24**, 4503-4509.
36. R. N. Mehta, M. Chakraborty, P. Mahanta and P. A. Parikh, *Industrial & Engineering Chemistry Research*, 2010, **49**, 7660-7665.
37. I. M. Rizwanul Fattah, H. H. Masjuki, M. A. Kalam, M. A. Wakil, H. K. Rashedul and M. J. Abedin, *Industrial Crops and Products*, 2014, **57**, 132-140.
38. M. Canakci, A. N. Ozsezen and A. Turkcan, *biomass and bioenergy*, 2009, **33**, 760-767.
39. J. B. Heywood, McGraw-Hill, Singapore, 1988.
40. A. E. Atabani, T. M. I. Mahlia, H. H. Masjuki, I. A. Badruddin, H. W. Yussof, W. T. Chong and K. T. Lee, *Energy*, 2013, **58**, 296-304.
41. T. T. Kivevele, M. M. Mbarawa, A. Bereczky, T. Laza and J. Madarasz, *Fuel Processing Technology*, 2011, **92**, 1244-1248.
42. A. Sanjid, H. H. Masjuki, M. A. Kalam, S. M. A. Rahman, M. J. Abedin and S. M. Palash, *Journal of Cleaner Production*.
43. S. Sivalakshmi and T. Balusamy, *Fuel*, 2013, **106**, 106-110.
44. S. Imtenan, H. H. Masjuki, M. Varman, M. A. Kalam, M. I. Arbab, H. Sajjad and S. M. Ashrafur Rahman, *Energy Conversion and Management*, 2014, **83**, 149-158.
45. M. S. Koçak, E. Ileri and Z. Utlu, *Energy & fuels*, 2007, **21**, 3622-3626.
46. A. N. Ozsezen, M. Canakci and C. Sayin, *Energy & Fuels*, 2008, **22**, 2796-2804.
47. Y. H. Teoh, H. H. Masjuki, M. A. Kalam, M. A. Amalina and H. G. How, *SAE Technical Paper*, 2013, **2013-01-2679**.
48. H. Sharon, K. Karuppasamy, D. Soban Kumar and A. Sundaresan, *Renewable Energy*, 2012, **47**, 160-166.
49. S. Imtenan, M. Varman, H. H. Masjuki, M. A. Kalam, H. Sajjad, M. I. Arbab and I. M. Rizwanul Fattah, *Energy Conversion and Management*, 2014, **80**, 329-356.
50. D. H. Qi, H. Chen, L. M. Geng and Y. Z. Bian, *Renewable Energy*, 2011, **36**, 1252-1258.
51. S. R. Turns, *An introduction to combustion : concepts and applications*, 2nd edn., McGraw-Hill, Singapoor, 2000.

Table 1 GC operating Condition for determination of fatty acid composition

Item	Specification
Column	HP-INNOWax (Crossed-Linked PEG) 0.32 mm * 30 m, 0.25 µm
Injection volume	1 µL
Carrier gas	Helium, 83 kPa
Injector	Split/splitless 1177, full EFC control
Temperature	250 ^{0}C
Split flow	100 mL/min
Column 2 flow	Helium at 1 ml/min constant flow
Oven	210 ^{0}C isothermal
Column temperature	60 ^{0}C for 2 min 10^{0}C /min to 200 ^{0}C 5^{0}C /min to 240 ^{0}C Hold 240 ^{0}C for 7 min
Detector	250 ^{0}C, FID, full EFC control

Table 2 Fatty acid composition of AL biodiesel

FAME	Structure	Molecular weight	Formula	AL biodiesel (%)
Methyl palmitate	16:0	270.45	$CH_3(CH_2)_{14}COOCH_3$	13.9
Methyl palmitoleate	16:1	268.43	$CH_3(CH_2)_5CH=CH(CH_2)_7COOCH_3$	0.2
Methyl stearate	18:0	298.5	$CH_3(CH_2)_{16}CO_2CH_3$	15.1
Methyl oleate	18:1	296.49	$CH_3(CH_2)_7CH=CH(CH_2)_7COOCH_3$	40.3
Methyl linoleate	18:2	294.47	$CH_3(CH_2)_3(CH_2CH=CH)_2(CH_2)_7COOCH_3$	25.6
Methyl linolenate	18:3	292.46	$CH_3(CH_2CH=CH)_3(CH_2)_7COOCH_3$	0.2
Methyl archidate	20:0	326.56	$CH_3(CH_2)_{18}COOCH_3$	0.3
Total ester content				95.6
Monoglycerie content				0.32
Diglyceride content				0.08
Triglyceride content				0.12
Total glycerin				0.109
Free glycerin				0.003

Table 3 Equipment of fuel property test

Property	Equipment	Manufacturer	Standard	ASTM D6751	Accuracy

			method	limit	
Kinematic viscosity at 40 °C	SVM 3000-automatic	Anton Paar, UK	D7042	1.9–6.0	±0.35%
Density at 40 °C	SVM 3000-automatic	Anton Paar, UK	D7042	n.s.	0.0005 g/cm3
Flash point	Pensky-Martens flash point-automatic NPM 440	Normalab, France	D93	130 min	±0.1 °C
Oxidation stability	873Rancimat-automatic	Metrohm, Switzerland	EN 14112	3 h	±0.01 h
Lower heating value	C2000 basic calorimeter-automatic	IKA, UK	D240	n.s.	±0.1% of reading
Cloud point	Cloud and Pour point tester-automatic NTE 450	Normalab, France	D2500	Report	±0.1 °C
Pour point	Cloud and Pour point tester-automatic NTE 450	Normalab, France	D97		±0.1 °C
Acid value	G-20 Rondolino automated titration system	Mettler Toledo, Switzerland	D664	0.5 max	±0.001 mg KOH/g

Table 4: Engine testbed equipment specification

Description	Specification

No. and arrangement of cylinders	4 in-line, longitudinal
Rated Power	65 kW at 4200 rpm
Combustion chamber	Swirl chamber
Total displacement	2477 cc
Cylinder bore x stroke	91.1 x 95 mm
Valve mechanism	SOHC
Compression ratio	21:1
Lubrication system	Pressure feed, full flow filtration
Fuel system	Distributor type injection pump
Air flow	Turbocharged
Fuel Injection Pressure	157 bar
Dynamometer	Froude Hofmann eddy current dynamometer Max. Power:250kW Max. Torque: 1200 Nm Max. Speed: 6000 rpm
Fuel flow meter	Positive displacement flow meter

Table 5 Measurement accuracy and uncertainty

Measured quantity	Upper limit	Accuracy	Uncertainty (%)
Fuel flow	36 l/h	± 0.02 l/h	
Speed	6000 rpm	±2 rpm	
Power	250 kW	±0.02 kW	
Smoke opacity	100%	0.1%	±0.5%
CO	10.00 vol.%	0.02 vol%	±0.01 vol%
HC	9999 ppm vol	1 ppm vol	±1 ppm
NO	5000 ppm vol	1 ppm vol	±5 ppm

Table 6 Property of the base fuels

Property	Unit	Diesel	AL biodiesel	*n*-butanol[c]	ASTM D6751[a]	EN 14214[b]

Kinematic Viscosity at 40^{0}C	mm^2/s	3.46	4.71	3.00	1.9-6.0	3.5-5.0
Density at 40^{0}C	Kg/m^3	829.6	868.6	812	n.s.	n.s.
Lower heating value	MJ/kg	44.66	39.38	34.33	n.s.	n.s.
Flash Point	^{0}C	69.5	141.5	35	130 (min)	120 (min)
Cloud Point	^{0}C	8	10	-	report	n.s.
Pour Point	^{0}C	7	8	-89	n.s.	n.s.
Acid value	Mg KOH/g	-	0.3	-	0.5 (max)	0.5 (max)
Saponification number (SN)	-	-	191.6	-	n.s.	n.s.
Iodine value (IV)	G I_2/100 g	-	82.1	-	n.s.	120
Cetane number (CN)	-	48[c]	56.3	~25	47 (min)	51 (min)

n.s. = not specified
[a]Data obtained from[40]
[b]Data obtained from[41]
[c]Provided by the supplier, measured at 20^0 C

Table 7 Property of the fuel blends

Property	Unit	AL20	AL15B5	AL10B10
Kinematic viscosity at 40 °C	mm^2/s	3.60	3.29	3.18
Density at 40 °C	Kg/m^3	837	834	831
Lower heating value MJ/kg	MJ/kg	43.69	43.40	43.15
Flash point	^{0}C	77.5	67.5	61.5
Cloud point	^{0}C	8	6	6
Pour point	^{0}C	4	2	2

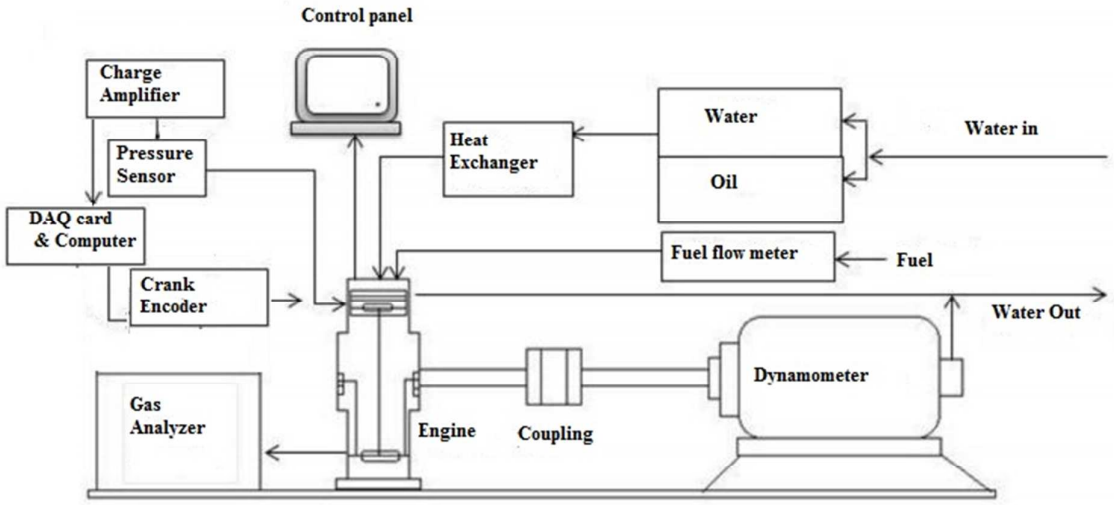

Figure 1: Schematic diagram of the engine test bed

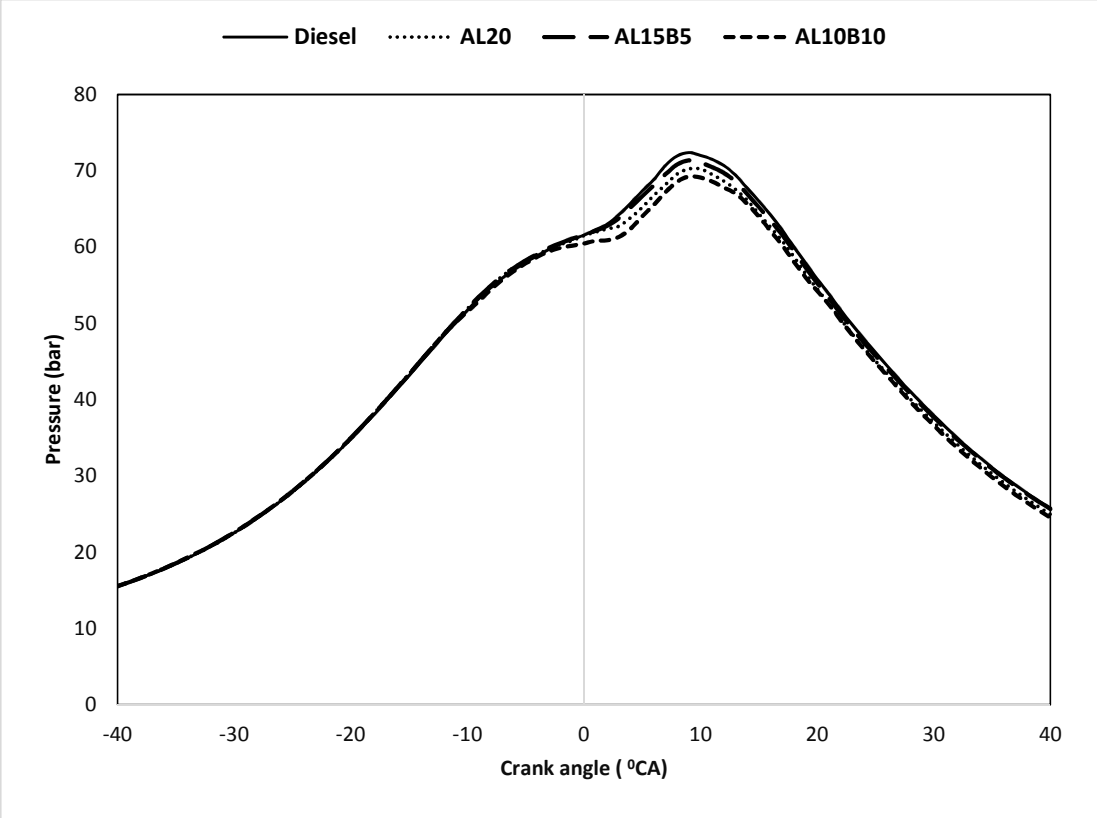

Figure 2 Cylinder pressure vs Crank angle diagram for *n*-butanol blends at 2000 rpm

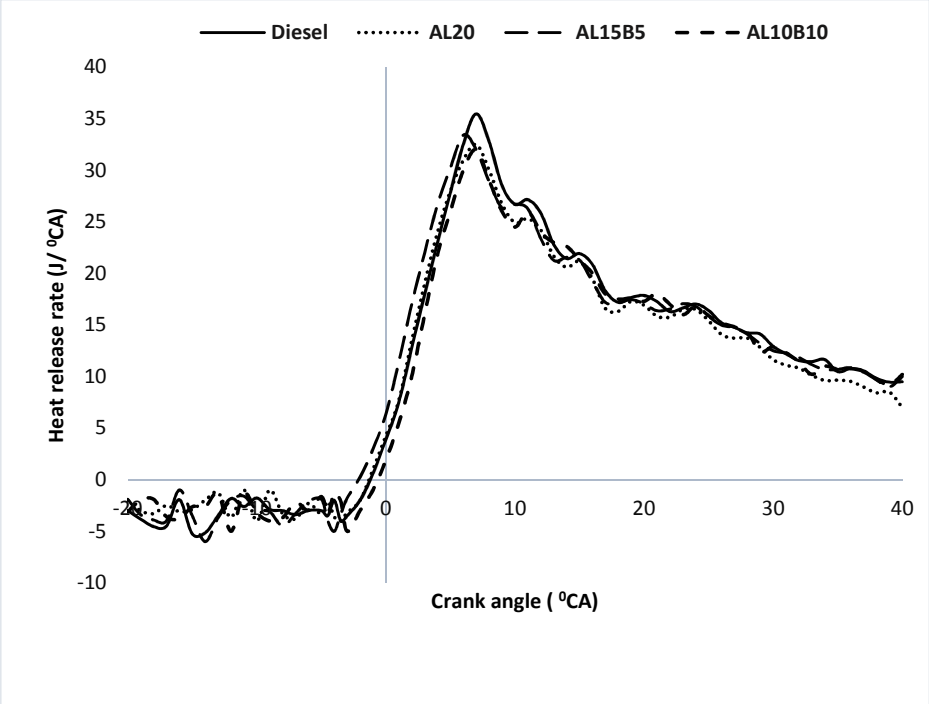

Figure 3 Heat release rate vs Crank angle diagram for *n*-butanol blends at 2000 rpm

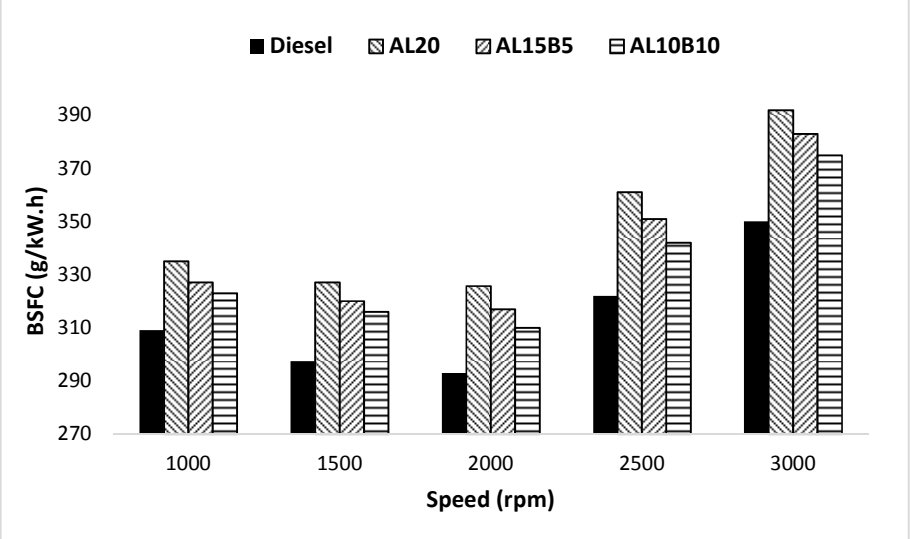

Figure 4 BSFC vs speed diagram for AL biodiesel and its modified blends at 80 Nm torque

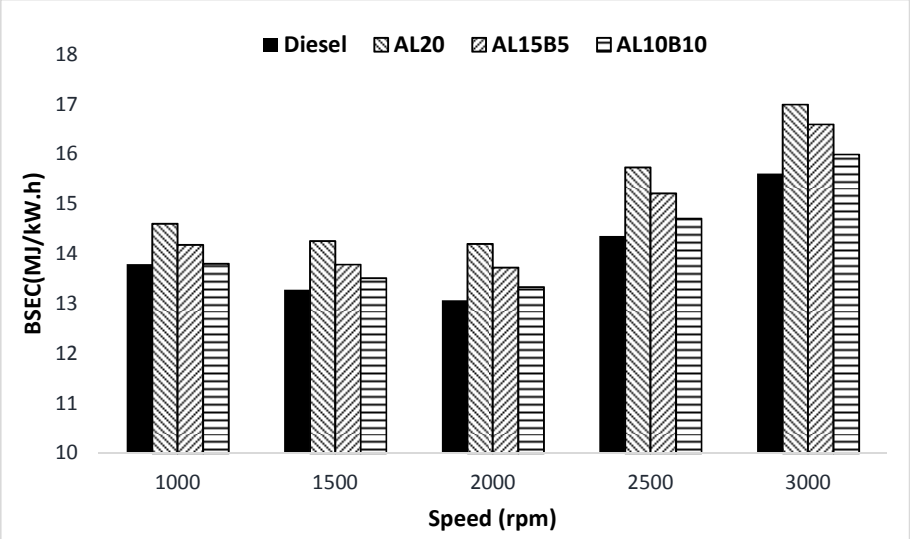

Figure 5 BSEC vs speed diagram for AL biodiesel and its modified blends at 80 Nm torque

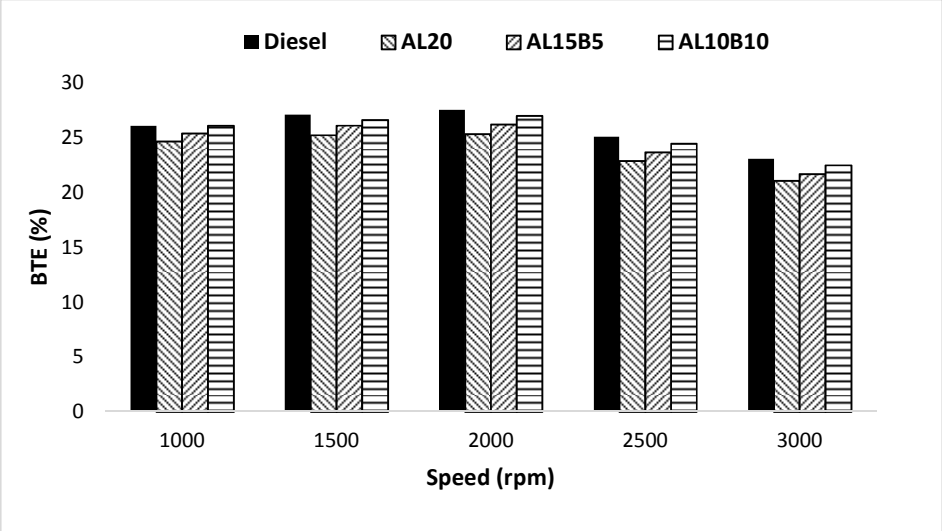

Figure 6 BTE vs speed diagram for AL biodiesel and its modified blends at 80 Nm torque

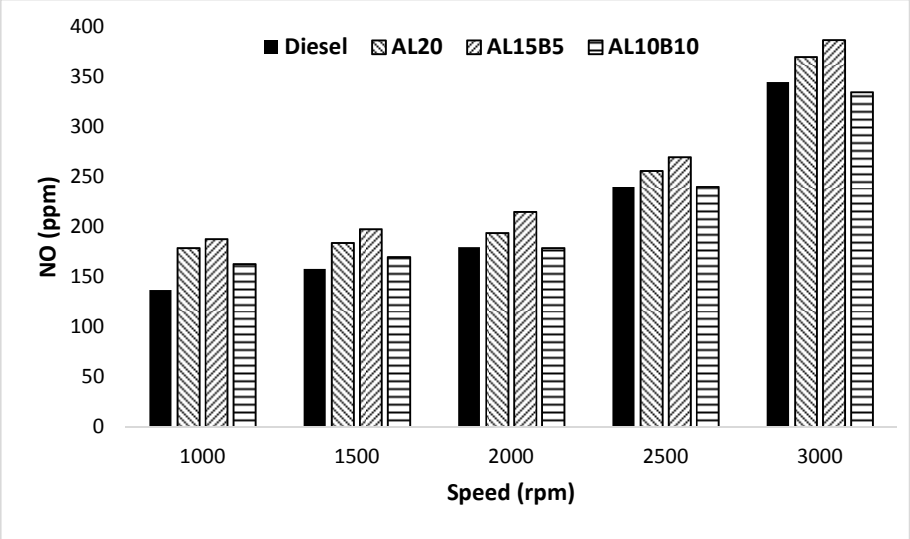

Figure 7 NO emission vs speed diagram for AL biodiesel and its modified blends at 80 Nm torque

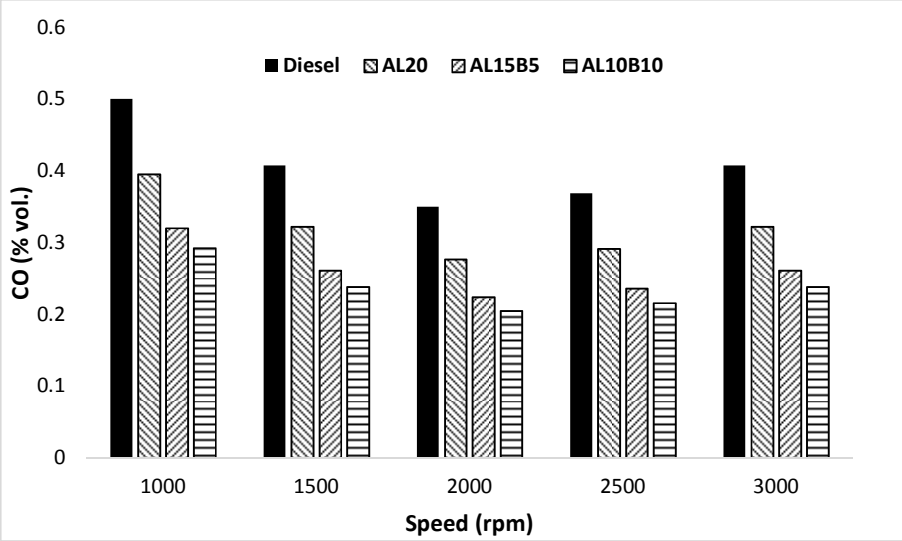

Figure 8 CO emission vs speed diagram for AL biodiesel and its modified blends at 80 Nm torque

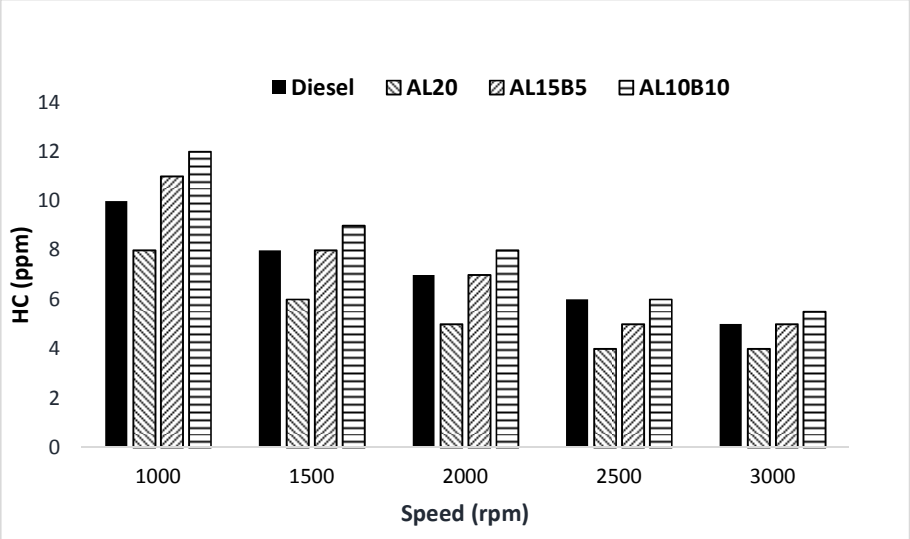

Figure 9 HC emission vs speed diagram for AL biodiesel and its modified blends at 80 Nm torque

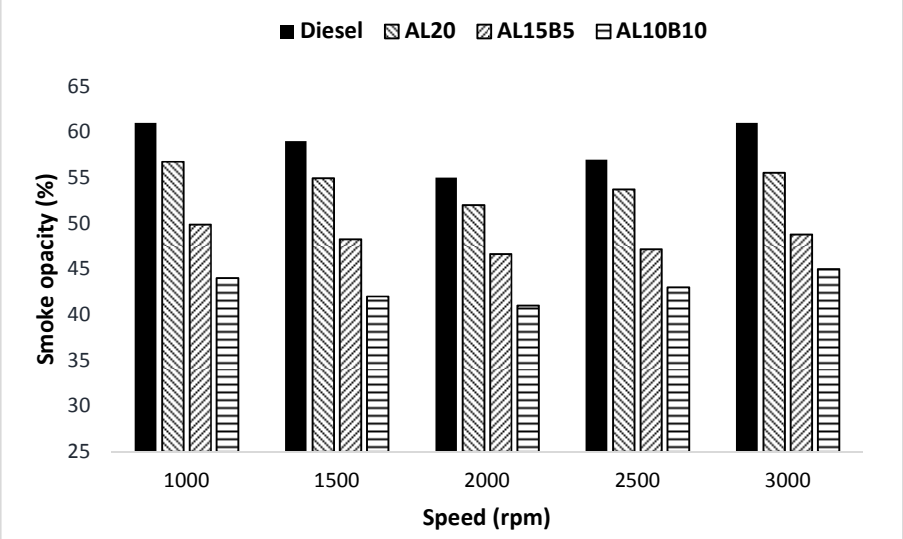

Figure 10 Smoke opacity vs speed diagram for AL biodiesel and its modified blends at 80 Nm torque